Materials Science in Semiconductor Processing 28 (2014) 135–143

Contents lists available at ScienceDirect

Materials Science in Semiconductor Processing

journal homepage: www.elsevier.com/locate/mssp

On the electrical characteristics of the Al/rhodamine-101/*p*-Si MS structure at low temperatures

Şükrü Karataş [a,*], Muzaffer Çakar [b], Abdülmecit Türüt [c]

[a] Kahramanmaraş Sütçü İmam University, Faculty of Sciences and Arts, Department of Physics, 46100 Kahramanmaraş, Turkey
[b] Kahramanmaraş Sütçü İmam University, Faculty of Sciences and Arts, Department of Chemstry, 46100 Kahramanmaraş, Turkey
[c] Physics Engineering Department, Faculty of Science, Istanbul Medeniyet University, Istanbul 34100, Turkey

ARTICLE INFO

Available online 4 September 2014

Keywords:
Organic/inorganic semiconductor structures
Barrier inhomoheneities
Si
I–V–T characteristics

ABSTRACT

In this paper, the current–voltage (*I–V*) characteristics of Al/Rhodamine-101/*p*-Si/Al metal–semiconductor (MS) structures have been measured at temperatures ranging from 80 to 325 K. The nonpolymeric organic compound rhodamine-101 (Rh101) film on a *p*-type Si substrate has been formed by means of the evaporation process and the Sn/rhodamine-101/Si contacts have been fabricated. The current–voltage characteristics of the diode show rectifying behaviour consistent with a potential barrier formed at the interface. The obtained *I–V* barrier heights (Φ_b) were in the range of 0.287–0.820 eV with ideality factors (n) of 6.31–2.68. The high values of ideality factor (n) may be ascribed to decrease of the exponentially increase rate in current due to space-charge injection into Rh101 thin film at higher voltage. The temperature-dependent *I–V* characteristics of the Al/Rhodamine-101/*p*-Si/Al structure have shown a Gaussian distribution giving mean barrier height of 0.918 eV and standard deviation of 0.104 V. The mean barrier height ($\overline{\Phi}_{bo}$) and the Richardson constant (A^*) values were obtained as 1.046 eV and 31.87 A K^{-2} cm^{-2}, respectively, by means of the modified Richardson plot, ln $[(I_0/T^2)-(q^2\sigma_0^2/2k^2T^2)]$ plot $1/kT$. The value of Richardson constant A^* obtained from this plot is approximately the same with theoretical value of 32 A cm^{-2} K^{-2} for *p*-Si. As a result, it can be concluded that the temperature dependent characteristic parameters for Al/Rhodamine-101/*p*-Si structure can be successfully explained on the basis of TE mechanism with Gaussian distribution of the barrier height

1. Introduction

Conducting polymers have been the subject of basic research over several years [1–3]; their properties e.g. stability, electronic structure make them suitable for commercial applications in electronic devices. However, up to now, the conducting or semiconducting polymers have by far not succeeded in challenging the inorganic materials in this field. But, in recent years there has been growing interest in the field of thin organic semiconducting films due to their successful application in optical and electronic devices. All plastic electronic devices such as organic thin film transistors, printable circuits, organic capacitors, and organic photovoltaic devices have received considerable attention in the past few years [4–9]. In particular, considerable attention was given in recent years to the preparation and properties of junctions or organic polymers with metals and inorganic semiconductors. The popularity of such studies, which is rooted in their importance to the semiconductor industry, does not assure uniformity of the results or of the interpretation. The polymer electronics has attracted considerable interest in

* Corresponding author. Tel.: +90 344 280 14 28; fax: +90 344 280 13 52.
E-mail address: skaratas@ksu.edu.tr (Ş. Karataş).

http://dx.doi.org/10.1016/j.mssp.2014.08.013

the recent years with the discovery of conducting polymers which could be used as active components in electronic devices [10,11]. Furthermore, organic semiconducting materials have now reached the early stages of commercialization with the technological success of thin-film organic optoelectronic devices, particularly organic light-emitting devices and by improving their efficiency, manufacturing yield and long-term stability [12–14]. The great advantage of organic semiconductors is that they are easy to fabricate directly from solution and in contrast to inorganic semiconductors do not need surfaces with regularity at the atomic level; because they do not have dangling bonds [15,16]. For that reason, there are a vast number of reports of experimental studies of metal/semiconductor systems

In spite of the recent technological success of these materials, relatively little is a detailed understanding of the charge injection and transport processes in organic semiconductor devices and therefore the analyzing these processes is crucial as mentioned in Refs. [12,17,18]. As mentioned above, due to the technological importance of metal–semiconductor devices in the electronics industry, contact properties of organic-semiconductor structures, such as polymer/inorganic semiconductor have been extensively studied [12,19]. But very little experimental studies are available on *I–V* characteristics of organic-semiconductor structures as a function of temperature. Some researchers have studied the electronic structures of various metals/organic interfaces by using various surface-scientific methods and the formation of an electric double layer and chemical interaction at the interface [20,21]. Tautz et al. [22] and Schwieger et al. [23], Hill et al. [24] and Peisert et al. [25] have presented a systematic study of the energy level alignment at the interfaces between metals and organic semiconductors, and have shown that there are contributions to the potential drop (dipole) across the metal/organic interface and a modification of the metal work function due to the adsorption of the organic molecules and a potential change in the organic semiconductor, respectively. Ahmad and Sayyad [26] and Veary-Roberts and Evans [27] have been recently made for the barrier height (BH) enhancement or modification using the thin organic interfacial layers. Sharma et al. [28] have studied the *I–V* characteristics in dark as well as under illumination and *C–V* characteristics in dark of the sandwich devices. That is, the electrical and photoelectrical properties of polymeric and nonpolymeric organic compounds have been investigated for more than the last two or three decades [29–31].

In diode parameters, such as ideality factor, barrier height, and series resistance affect the performance of the device. These parameters give useful information concerned with the nature of the diode. The classical model of Schottky diode assumes the junction to be abrupt with a fixed barrier height. The analyses of the current–voltage (*I–V*) characteristics of the Schottky diodes obtained only at room temperature showed that it does not give detailed information about the charge transport process and about the nature of the barrier formed at the metal–semiconductor interface, i.e. it is necessary to determine the diode parameters over a wide range of temperature at metal/semiconductor or polymer/inorganic semiconductor contacts to understand the nature of barrier and conduction mechanism. Because, the temperature dependence of the *I–V* characteristics allows us to understand different aspects of conduction mechanisms [9,32,33]. The observed current–voltage characteristics of the real Schottky barrier diode usually deviate from the ideal thermionic emission (TE) model. The strong dependence of both barrier height and ideality factor on temperature and the nonlinearity of the Richardson plots are the factors associated with the deviation from the TE model [34–37]. The decrease in barrier height at low temperature leads to non-linearity in the activation energy of $\ln(I_0/T^2)$ versus $(kT)^{-1}$ plot. The deviation in TE model observed in *I–V* characteristics could be quantitatively explained by assuming specific distribution of nanometer scale patches of small regions with low barrier heights embedded in a high uniform barrier height background [38–42].

In the present study, we have used rhodamine-101 as an interlayer for the modification of Al/Si (100) Schottky contacts, where the rhodamine-101 will be called the Rh101, and we have formed Al/Rh101/*p*-Si contacts which show rectifying contact behavior. The rhodamine-101 is a xanthene's type molecule and has a quantum yield in ethanol close to unity, being independent of temperature [43,44]. Its appearance is green solid. The temperature dependence of the experimental forward bias current–voltage characteristics of the Al/Rhodamine-101/*p*-Si/Schottky structure were investigated at low temperatures.

2. Experimental techniques

The samples were prepared using cleaned and polished *p* type Si wafers with (100) orientation and 5–10 Ω-cm resistivity. The RCA cleaning procedure was as follows: a 10 min boil in $NH_3+H_2O_2+6H_2O$ followed by a 10 min boil in $HCl+H_2O_2+6H_2O$. The RCA cleaning with HF dip shows a predominant coverage of the surface with hydride groups. All contact metals were cleaned by acetone and methanol before the processes. The ohmic contact was made by evaporating Al on the back surface of the *p*-type Si substrate. Al plus *p*-Si system at 580 °C for 3 min in N_2 atmosphere to form a heavily doped *p*-type region ($p+$) [22]. The native oxide on the front surface of the substrates was removed in HF:H_2O (1:10) solution and finally the wafers were rinsed in de-ionized water for 30 s before forming the Rh101 organic layer on the front surfaces of the substrates. Then the substrates were inserted into the vacuum system of 10^{-5} Torr, and the Rh101 was evaporated on the front surface of the substrates by using a resistance heater. The Rh101 was evaporated on the surface of *p*-type Si semiconductor in electrolyte solution under the condition of constant temperature of 30 °C. The Rh101 organic layer with a thickness of 40 nm was directly formed on the front surface of the *p*-Si wafer [9]. The deposition rate of the Rh101 was between 6 and 9 nm/s, as determined using a quartz-crystal thickness monitor. The distance from the evaporation source to the Si substrates was maintained at 12 cm and the substrate temperature was about 30 °C. Finally, top metal contact, Al, was deposited (as rectifying metal) on the Rh101/*p*-Si/Al structure through a shadow mask. Thus, the Al/Rh101/*p*-Si/Al structure was obtained. The area of the circular

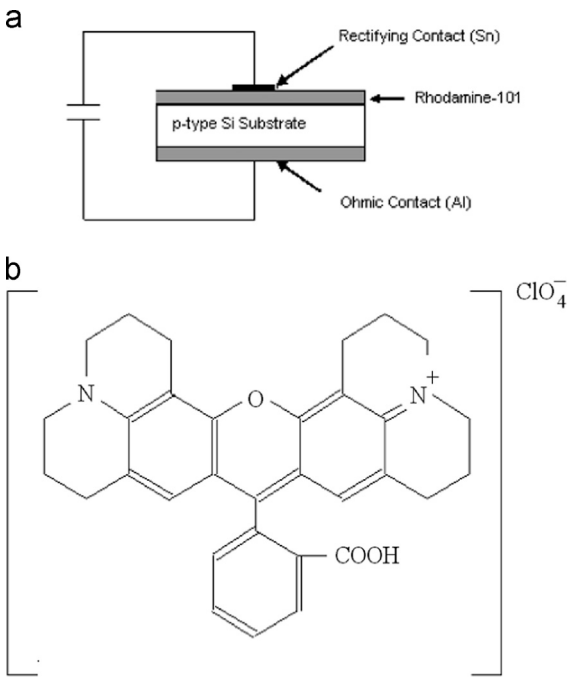

Fig. 1. (a) Cross-section of the studied structure; (b) molecular structure of the Rhodamine-101 (molecular formula: $C_{32}H_{31}N_2O_7Cl$).

rectifying contacts was 1.767×10^{-2} cm^2. All contact metals were cleaned by acetone and methanol before the processes. Furthermore, cross-section of the studied structure, and molecular structure of the Rhodamine-101 are given in Fig. 1(a) and (b), respectively.

The *I–V* characteristics of the devices were measured in the temperature range of 80–325 K using a temperature controlled janes vpf-475 cryostat, which enables us to make measurements in the temperature range of 77–450 K, and a Keithly 220 programmable constant current source and a Keithly 199 dmm/scanner under dark conditions. The sample temperature was always monitored by using a copper-constantan thermocouple and a lakeshore 321 auto-tuning temperature controller with sensitivity better than ±0.1 K. All measurements were carried out with the help of a microcomputer through an IEEE-488 ac/dc converter card.

3. Results and discussion

3.1. Temperature dependence of the forward bias current–voltage (I–V) characteristics

The forward current–voltage characteristics of Al/Rh-101/*p*-Si Schottky diodes in the temperature range of 80–325 K are shown in Fig. 2. The current–voltage (*I–V*) characteristics are one of the methods to determine the some electrical properties in diodes. The current–voltage characteristics due to thermionic emission of a non-ideal Schottky diode can be expressed as [45];

$$I=I_0\exp\left(\frac{qV}{nkT}\right)\left[1-\exp\left(-\frac{qV}{kT}\right)\right] \quad (1)$$

where

$$I_0=A\ \ A^*\ T^2\ \exp\left(-\frac{q\Phi_b}{kT}\right) \quad (2)$$

I_0 is the saturation current derived from the straight line intercept of ln *I* axis at zero bias ($V=0$), n is the ideality factor which introduced to take into account the deviation of the experimental *I–V* data from the ideal thermionic model and should be $n=1$ for an ideal contact

From Eqs. (1) and (2), the ideality factor n and barrier height $\Phi_b(I\text{–}V)$ can be written respectively as;

$$n=\frac{q}{kT}\frac{dV}{d\ln(I)} \quad (3)$$

$$\Phi_b=\frac{kT}{q}\ln\left(\frac{AA^*T^2}{I_0}\right) \quad (4)$$

where A^*, A, Φ_b, q and k are the Richardson constant (32 A cm^{-2} K^{-2} for *p*-type Si), the Schottky contact area, the Schottky barrier height, the electron charge and the Boltzman constant, respectively. Putting these values in Eqs. (3) and (4), the values of idealite factors and Schottky barrier heights (SBH) were calculated. The barrier height and ideality factor versus temperature are shown in Fig. 3. As can be seen Fig. 3, the values of idealite factor and barrier heights (Φ_b) determined from the forward *I–V* plots were found to be a strong function of temperature. The experimental values of Φ_b and n for Al/Rh-101/*p*-Si Schottky structure was measured in the range from 0.286 eV and 6.31 (at 80 K) to 0.820 eVand 2.68 (at 325 K), respectively. In Eq. (3), $n=1$ for an ideal diode. However, n has usually a value greater than unity. High values of n can be attributed to the presence of the interfacial thin native oxide layer, series resistance, etc. But, the barrier inhomogeneities have been very important explanation for the higher values of the ideality factor. As expected, while Φ_b increases with increase in temperature, n decreases. When the temperature increases, more and more electrons have sufficient energy to surmount the higher barrier. Since current transport across the metal–semiconductor interface is a temperature activated process, electrons at low temperatures are able to surmount the lower barriers and therefore current transport will be dominated by current flowing through the patches of lower barrier height [37,45–47]. As a result, the dominant barrier height will increase with the temperature and bias voltage [47]. Therefore, the current flow through the lower barrier height and a larger ideality factor will dominate current transport. However, a value of 0.784 eV for the Al/Rh101/*p*-Si/Al Schottky structure was obtained at the room temperature that is significantly larger than the value of 0.58 eV of the conventional *p*-Si Schottky structure [45,46]. The obtained barrier height of 0.784 eV (at room temperature) is a priori independent of temperature, and is higher than the values obtained for TE. It is also much higher than barrier height values of 0.4–0.7 eV obtained usually for *p*-type Si independent of the Schottky metal. It should be known that Φ_b is the contact potential barrier that exists at the interface between the polymeric organic and inorganic layers, i.e. at the rhodamine-101/*p*-Si interface. In the other words, at high current densities,

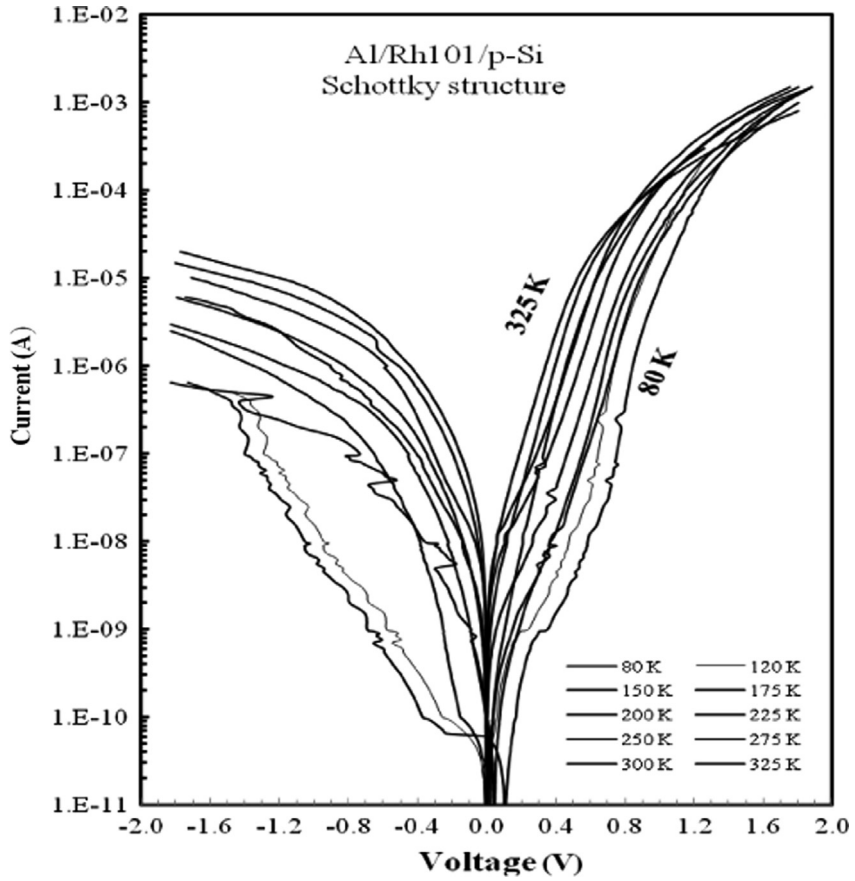

Fig. 2. The current–voltage characteristics of Al/Rho-101/*p*-Si Schottky structure in the temperature range of 80–325 K.

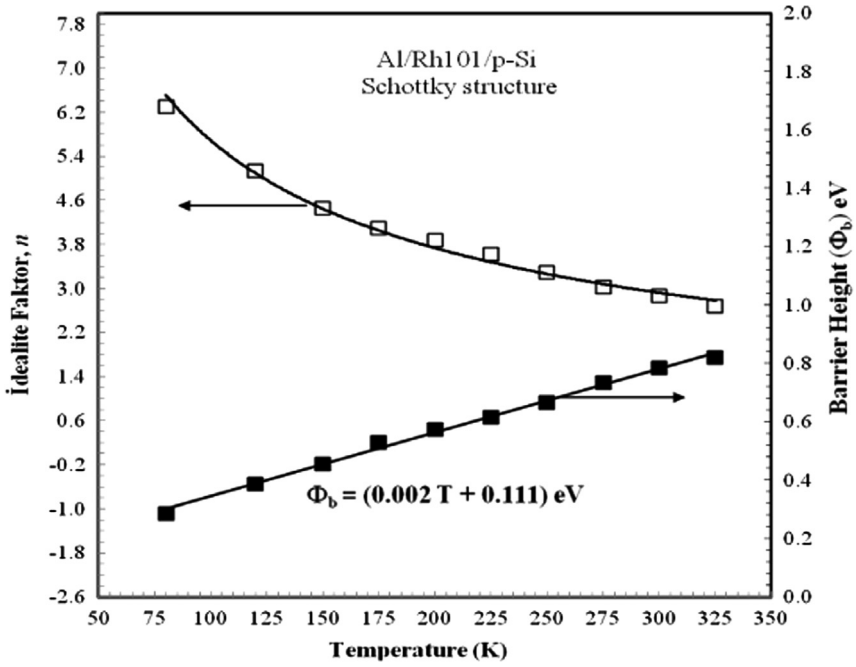

Fig. 3. Temperature dependence of the ideality factor and the experimental barrier height Φ_b for the Al/Rho-101/*p*-Si Schottky structure.

a space-charge injection can be proceed through the Rh101/*p*-Si heterostructure from the *p*-Si into the organic layer (the Rh101 layer), that is, in this case, the current is called the space charged limited current (SCLC) [48–50]. Thus, the SCLC conduction should become important when the density of injected free-charge carriers is much larger than the thermal-generated free-charge-carrier density. Thus, the SCLC conduction should become important when the density of injected free-charge carriers is much larger than the thermal-generated free-charge-carrier density.

Fig. 4 shows the experimental barrier heights versus the ideality factors plot of the Al/Rh101/*p*-Si Schottky structure in the temperature range in temperatures ranging from 80 to 325 K. Schmitsdorf et al. [51] used Tung's [52] theoretical approach and they found a linear correlation between the experimental zero-bias barrier heights (Φ_b) and the ideality factors (n). As can be seen from Fig. 4, there is a linear relationship between the experimentally effective barrier heights (BHs) and the ideality factors (n) of the Al/Rh101/*p*-Si Schottky barrier diodes (SBDs) that is explained by lateral inhomogeneities of the barrier heights in the SBDs [51]. The extrapolation of the experimental BHs versus ideality factors plot to $n=1$ has given a homogeneous BH of approximately 0.978 eV. The other barrier height values deviate from this value due to local inhomogeneities. The homogeneous BH value of 0.978 eV is in agreement with values 0.940 and 0.933 eV obtained in our previous studies [12,50].

The thermionic emission (TE) theory is normally used to extract the Schottky diode parameters [53–55]. However, there have been reports about a deviation from this classical TE theory [53,56,57] especially at low temperature. It was found to increase, while the barrier height decreases with decreasing temperature [57] and this behavior leads to nonlinearity in the activation energy plot in the whole temperature range. Thus, we show the conventional energy variation of $\ln(I_0/T^2)$ versus $1/T$ or $1/nT$ (Fig. 5) for the Al/Rh101/*p*-Si Schottky barrier diodes. The saturation current density for $V=0$, which is used for the Richardson plot, can be written as

$$\ln\left(\frac{I_o}{T^2}\right) = \ln(AA^*) - \frac{q\Phi_{bo}}{nkT} \tag{5}$$

where A^* is the Richarson constant and Φ_{bo} is the mean zero voltage barrier height. According to the TE theory, the slope of the conventional Richardson plot [$\ln(I_0/T^2)$ versus $1/kT$ plot] should give the barrier height Φ_{bo}. However, the experimental data obtained in this study do not correlate well with a straight line below 175 K. For the evaluation of the BH, one may also use Richardson plots from saturation currents. Fig. 5 shows a conventional activation energy ln (I_0/T^2) vs. $1/kT$ plot (indicated by open squares) according to TE theory [39] for Al/Rh101/*p*-Si Schottky diode. Experimental $\ln(I_0/T^2)$ versus $1/kT$ plot shows a significant deviation from linearity at low temperatures (in below 175 K), whereas the plot of $\ln(I_0/T^2)$ versus $1/nkT$ (open triangles) is linear in the temperature range 80–325 K with a slope giving an activation energy of 1.22 eV. The experimental data for $1/kT$ plot are seen to be fitted asymptotically to a straight line at higher temperatures only. The activation energy value from the slope of this straight line

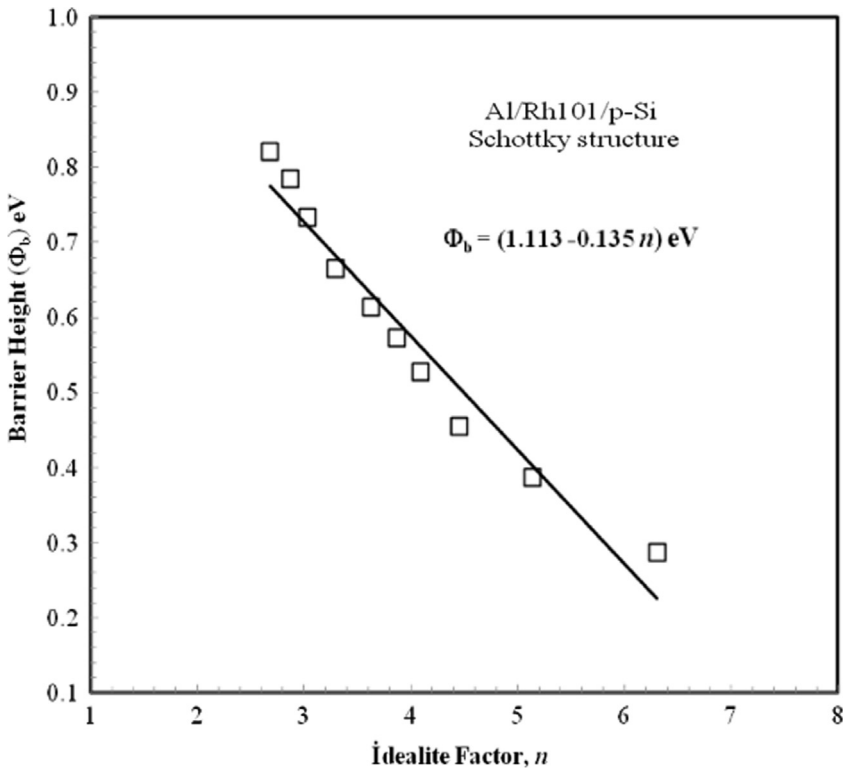

Fig. 4. Linear variation of barrier height versus ideality factors in the temperature range of 80–325 K for the Al/Rho-101/*p*-Si Schottky structure.

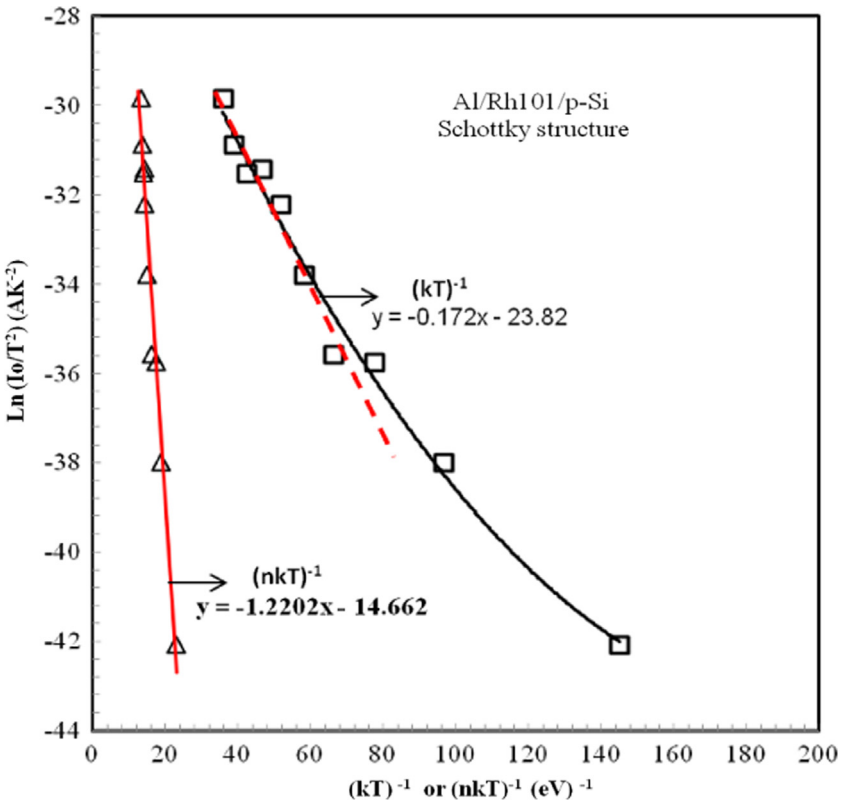

Fig. 5. Conventional activation energy ($\ln(I_0/T^2)$ versus $1/kT$) plot (the open squares) and ($\ln(I_0/T^2)$ versus $(1/nkT)$) plot (the open triangles) for the Al/Rho-101/*p*-Si Schottky structure.

has been obtained as 0.17 eV for $1/kT$ (Fig. 5). Bowing of the experimental $\ln(I_0/T^2)$ versus $1/kT$ curve may be caused by the temperature dependence of the BH and ideality factor due to the existence of the surface inhomogeneities of the Si substrate [45,46,55,58]. Also, the deviation in the Richardson plots may be due to the spatially inhomogeneous BHs and potential fluctuations at the interface that consist of low and high barrier areas [58–62]. That is, the current through the diode will flow preferentially through the lower barriers in the potential distribution. Furthermore, the nonlinear behavior of the $\ln(I_0/T^2)$ versus $1/kT$ plot at low temperatures is caused by apparent reduction arising from the laterally inhomogeneous of the barrier height. The Richardson constant value of $A^*=2.44\times10^{-5}\,\mathrm{A\,cm^{-2}\,K^{-2}}$ was determined from the intercept at the ordinate of the experimental plot. This value is much lower than the known value of the Richardson constant for electrons in *p*-type Si ($32\,\mathrm{A\,cm^{-2}\,K^{-2}}$) [45,46]. It can be seen very low values of Richardson constant in literature for inhomogeneous barrier such as in Refs. [11,63]. At the same time, the deviation in the Richardson plots may be due to the spatially inhomogeneous BHs and potential fluctuations at the interface that consists of low and high barrier areas, that is, the current through the diode will flow preferentially through the lower barriers in the potential distribution. As was explained by Horvath [64], the value of A^* obtained from the temperature dependence of the *I–V* characteristics may be affected by the lateral inhomogeneity of the barriers, and the fact that it is different from the theoretical value may be connected to a value of the real effective mass that is different from the calculated one.

The abnormal behavior of current–voltage characteristics of a Schottky barrier diode has been attributed to the spatial variation of barrier heights (BHs). Lately, the nature and origin of the decrease in the BH and increase in ideality factor with a decrease in temperature in some studies [12,35,52,65] have been successfully explained on the basis of a thermionic emission mechanism with Gaussian distribution of the BHs, due to the barrier height inhomogeneities prevailing at the MS interface. Song et al. [35] have introduced an analytical potential fluctuation model (a Gaussian distribution of the BHs). Thus, the above abnormal behaviors can be explained using an analytical potential fluctuation model based on spatially inhomogeneous BHs at the interface [33,35,54,66,67]. This model is based on spatially inhomogeneous BHs at the interface. Let us assume that the distribution of the BHs is a Gaussian distribution with a mean value $\overline{\Phi}_b$ and a standard deviation σ_s. The standard deviation is a measure of the barrier homogeneity. The total current in a given forward bias V is then given by

$$I(V)=I_0\exp\left(\frac{qV}{n_{ap}kT}\right)\left[1-\exp\left(-\frac{qV}{kT}\right)\right] \tag{6}$$

with

$$I_0=A\ \ A^*\ T^2\ \exp\left(-\frac{q\Phi_{ap}}{kT}\right), \tag{7}$$

where Φ_{ap} and n_{ap} are the apparent BH and the apparent ideality factor, respectively, which are given by

$$\Phi_{ap} = \overline{\Phi}_{bo} - \frac{q\sigma_0^2}{2kT} \tag{8}$$

$$\left(\frac{1}{n_{ap}} - 1\right) = \rho_2 - \frac{q\rho_3}{2kT}. \tag{9}$$

It is assumed that the mean SBH $\overline{\Phi}_b$ and σ_s are linearly bias dependent on Gaussian parameters, such as $\overline{\Phi}_b = \overline{\Phi}_{bo} + \rho_2 V$ and standard deviation $\sigma_s = \sigma_{so} + \rho_3 V$, where ρ_2 and ρ_3 are voltage coefficients and they quantify the voltage deformation of the BH distribution. Here, the temperature dependence of σ_s is usually small and can be neglected. Fitting of the experimental data in Eqs. (2) or (7) and in Eq. (4) provides Φ_{ap} and n_{ap}, respectively, which should obey Eqs. (8) and (9). Thus, the plot of Φ_{ap} versus $1/T$ (Fig. 6) should be a straight line that gives $\overline{\Phi}_{bo}$ and σ_0 from the intercept and slope, respectively. As can be seen in Fig. 6, the values of 0.918 eV and 0.104 V for $\overline{\Phi}_{bo}$ and σ_0 (the zero-bias standard deviation), respectively, were obtained from the experimental Φ_{ap} versus $1/T$. It was seen that the value of $\sigma_0 = 0.104$ V is not small compared to the mean value of $\overline{\Phi}_{bo} = 1.918$ eV, and it indicates the presence of the interface inhomogeneities. Nevertheless, this inhomogeneity and potential fluctuation dramatically affect low temperature *I–V* characteristics. It is responsible, in particular, for the curved behavior in the Richardson plot (in Fig. 5). In the same figure (in Fig. 6), the plot of nap versus $1/T$ should be a straight line that gives voltage coefficients ρ_2 and ρ_3 from the intercept and slope, respectively. The temperature dependence of the ideality factor can be understood on the basis of Eq. (9). Fitting showing ideality factor, n, in Fig. 6 is a straight line that gives voltage coefficients ρ_2 and ρ_3 from the intercept and slope of the plot where $\rho_2 = -0.04$ V and $\rho_3 = -0.556$ V from the experimental data. The linear behavior of this plot demonstrates that the ideality factor does indeed express the voltage deformation of the Gaussian distribution of the BH. Furthermore, the experimental results of nap fit very well with theoretical Eq. (9) using the values of the voltage coefficients. It was seen that the lower value of σ_0 corresponds to more homogenous barrier height. Therefore, Figs. 3 and 6 show that the temperature dependence of the experimental data of the Al/Rh101/*p*-Si contact is also in agreement with a Gaussian BH distribution model, that is, such a model may be able to explain the fluctuations but not the fundamental reason why the ideality factors are so high. Therefore, the thermionic emission-limited regime is clearly apparent from the region where the current increases exponentially with applied voltage [12,44,68]. At higher voltage, the rate of increase in current decreases due to space-charge injection into Rh101 thin film, that is, the *I–V* characteristics are influenced by the transport properties of the organic material. As conclusion, the transport through the organic thin film is governed by space charged limited current.

Due to the barrier inhomogeneity at low temperatures, the conventional Richardson plot deviates from linearity. Thus, as mentioned above, the activation energy plot, [$(\ln(I_0/T^2)$ versus $1/kT$], shows nonlinearity at low temperatures. To explain these discrepancies according to the Gaussian distribution of the BH, for a modified activation energy plot, Eq. (7) can be rewritten by combining with Eq. (9) as;

$$\ln\left(\frac{I_0}{T^2}\right) - \left(\frac{q^2\sigma_s^2}{2k^2T^2}\right) = \ln(AA^*) - \frac{q\overline{\Phi}_{bo}}{kT} \tag{10}$$

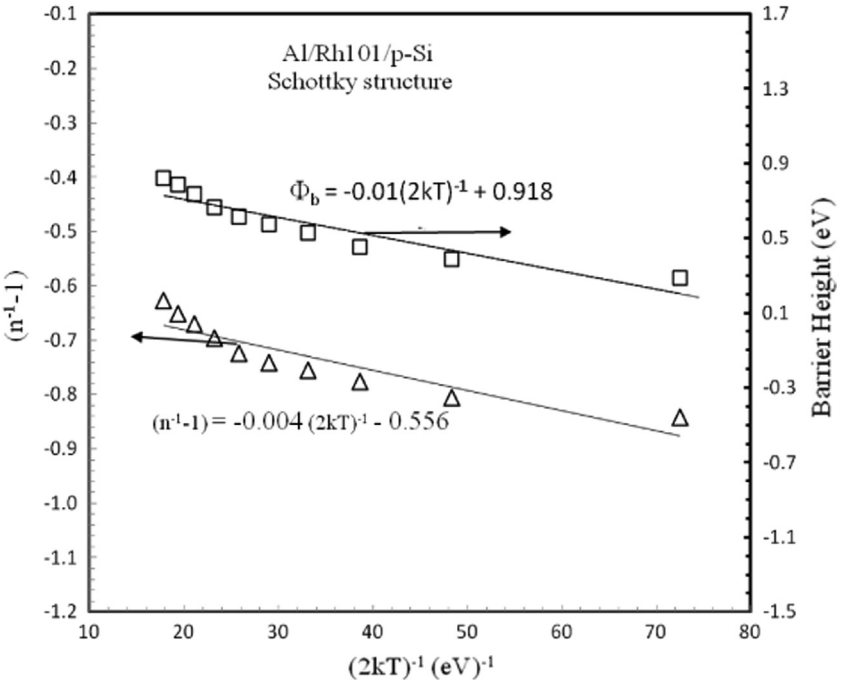

Fig. 6. The barrier height Φ_{ap} (the open squares) obtained from *I–V* measurements as a function of inverse temperature and the inverse ideality factor $1/n_{ap}$ (the open triangles) versus inverse temperature ($1/2kT$) plot for the Al/Rho-101/*p*-Si Schottky structure.

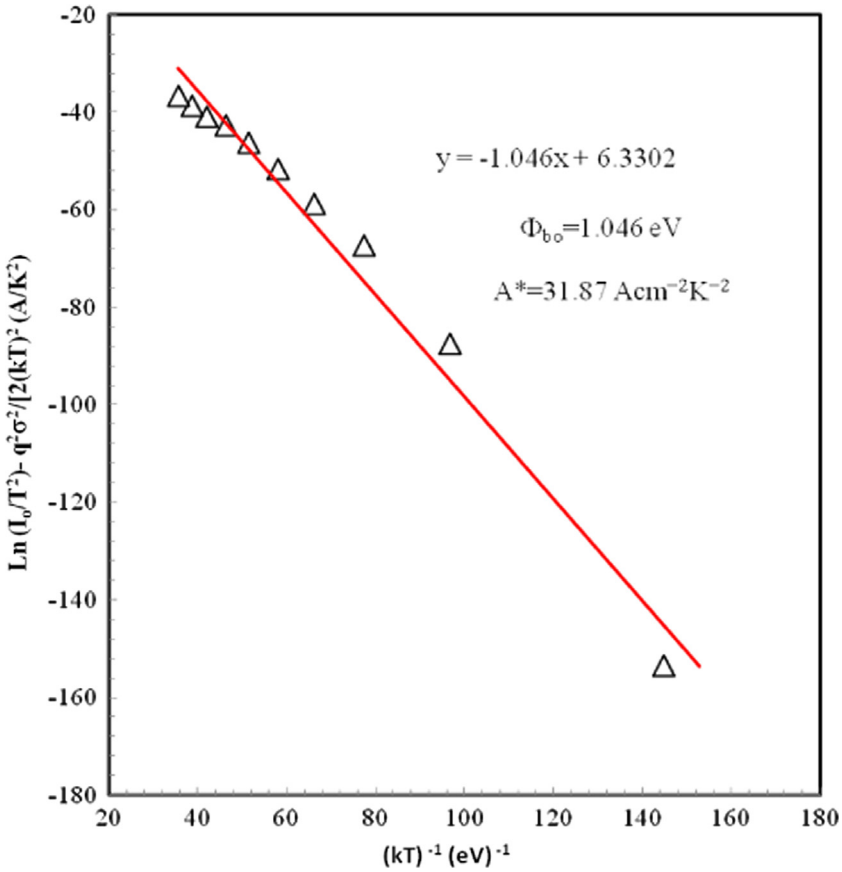

Fig. 7. Modified activation energy ($\ln(I_0/T^2)$–$q^2\sigma_0^2/2k^2T^2$ versus $1/kT$) plots for the Al/Rho-101/*p*-Si Schottky structure according to Gaussian distributions of barrier heights.

A modified $\ln(I_0/T^2)$–$q^2\sigma_0^2/2k^2T^2$ versus $1/T$ plot according to Eq. (10) should give a straight line with the slope directly yielding the mean $\overline{\Phi}_{bo}$ and the intercept ($=\ln AA^*$) at the ordinate determining A^* for a given diode area A. Fig. 7 shows this plot. As shown in Fig. 7, the modified $\ln(I_0/T^2)$–$q^2\sigma_0^2/2k^2T^2$ versus $1/T$ plot gives as $\overline{\Phi}_{bo}=1.046$ eV and $A^*=31.87$ A cm^{-2} K^{-2}. As can be seen, the value $\overline{\Phi}_{bo}=1.046$ eV obtained from $\ln(I_0/T^2)$ $-q^2\sigma_0^2/2k^2T^2$ versus $1/T$ plot is closer to the value of $\overline{\Phi}_{bo}=0.918$ eV from Φ_{ap} versus $1/T$ plot in Fig. 6. In short, the homogeneous BH value 0.978 eV is agreement with values 0.940 and 0.933 eV obtained in our previous studies [12,50]. Furthermore, barrier height values obtained from different methods (from *I–V*, Richardson and Gaussian) are in agreement with each other. However, the Richardson constant value of 31.87 A cm^{-2} K^{-2} obtained from the modified Richardson plot is almost the same as with known value of holes with 32 A cm^{-2} K^{-2} in *p*-type Si.

4. Conclusions

In this study, the current–voltage (*I–V*) characteristics of the Al/Rh101/*p*-Si Schottky contact prepared by a vacuum coating technique were investigated in the temperature range of 80–325 K. The non-polymeric organic compound Rh101 interfaced to the inorganic *p*-Si provides the rectifying *I–V* characteristics. The obtained *I–V* BHs are in the range of 0.286–0.820 eV with ideality factor of 6.31–2.68. A value of 0.784 eV for the Al/Rh101/*p*-Si/Al Schottky structure was obtained at the room temperature that is significantly larger than the value of 0.58 eV of the conventional *p*-Si Schottky structure. Furthermore, the results are fitted to a model of a Gaussian distribution of the barrier heights to explain the fluctuations of the characteristic parameters, suggesting that the contacts are not spatially uniform. The laterally homogeneous SBH value of approximately 0.978 eV for the Al/Rh101/*p*-Si Schottky structure has been deduced from the linear relationship between the experimental BHs and ideality factors. It was shown that the *I–V* characteristics of the Al/Rh101/*p*-type Si Schottky structures can be interpreted on the basis of the TE mechanism with Gaussian distribution of the BHs of $\overline{\Phi}_{bo}=1.046$ eV and standard deviation of 0.104 V. The activation energy $\ln(I_0/T^2)$ versus $1/(nkT)$ plot yielded a straight line with an effective barrier height value of 1.22 eV. It has been seen that the analysis under the Gaussian distribution of BH model or n versus $1/T$ plot show a slope behavior and serve as the basis for the proposal of the presence of a double Gaussian distribution of BHs at the MS interface. It can be said that this Al/Rh101/*p*-Si Schottky contacts show good diode behavior. According to the electrical characterization, in the future, it can be used rectifying

contacts, integrated circuits, the other electronic devices and so on.

Acknowledgements

This work was supported by Kahramanmaraş Sütçü İmam University Commission of Scientific Research Projects under Grant No. 2013/4-24 M. The authors also thank to Kahramanmaraş Sütçü İmam University.

References

[1] CK Chiang, RR Fincher, YW Park, AJ Heeger, H Schirakawa, EJ Louis, et al., Phys. Rev. Lett. 39 (1977) 1098.
[2] TA Skothheim (Ed.), Handbook of Conducting Polymers, Marcel Dekker, New York, 1986.
[3] G. Appel, R. Mikalo, K. Henkel, A. Oprea, A. Yfantis, I. Paloumpa, D. Schmeiûer, Solid-State Electron. 44 (2000) 855.
[4] G.D. Sharma, Manmeeta, Dhiraj Saxena, M.S. Roy, Mater. Sci. Eng. B 79 (2001) 146.
[5] G. Yu, A.J. Heeger, J. Appl. Phys. 78 (1995) 4510.
[6] A.J. Campbell, D.D.C. Bradley, D.G. Lidzey, J. Appl. Phys. 82 (1997) 6327.
[7] C.J. Huang, S. Han, D. Groze, A. Turak, Z.H. Lu, J. Appl. Phys. 97 (2005) 086107.
[8] H. Bayhan, A.S. Kavasoglu, Solid-State Electron. 49 (2005) 991.
[9] Ş. Karataş, M. Çakar, Synth. Met. 159 (2009) 347.
[10] M.F. Ruber, in: G.J. Ashwell (Ed.), Molecular Electronics, Wiley, New York, 1992.
[11] Ş. Aydoğan, M. Sağlam, A. Türüt, Appl. Surf. Sci. 250 (2005) 43–49.
[12] Ş. Karataş, C. Temirci, M. Çakar, A. Türüt, Appl. Surf. Sci. 252 (2006) 2209.
[13] C.D.J. Blades, A.B. Walker, Synth. Met. 335 (2000) 111.
[14] S.R. Forrest, Chem. Rev. 97 (1997) 1793.
[15] Ş. Aydoğan, M. Sağlam, A Türüt, Polymer 46 (2005) 6148.
[16] P. Stallinga, H.L. Gomes, H. Rost, A.B Holmes, M.G. Harrison, R.H. Friend, F. Biscarini, C. Taliani, G.W. Jones, D.M. Taylor, Physica B 923 (1999) 273.
[17] W. Brutting, S. Berleb, A.G. Muckl, Org. Electron. 2 (2001) 1.
[18] M. Lonergan, Annu. Rev. Phys. Chem. 55 (2004) 257.
[19] Ş. Aydoğan, M. Sağlam, A Türüt, Y. Onganer, Synth. Met. 150 (2005) 15.
[20] H. Ishii, K. Sugiyama, E. Ito, K. Seki, Adv. Mater. 11 (1999) 605.
[21] K. Seki, N. Hayashib, H. Oji, E. Ito, Y. Ouchi, H. Ishii, Thin Solid Films 393 (2001) 298.
[22] F.S. Tautz, M. Eremtchenko, J.A. Schaefer, M. Sokolowski, V. Shklover, K. Glockler, E. Umbach, Surf. Sci. 176 (2002) 502.
[23] T. Schwieger, H. Peisert, M. Knupfer, Chem. Phys. Lett. 384 (2004) 197.
[24] I.G. Hill, A. Kahn, Z.G. Soos, R.A. Pascal Jr., Chem. Phys. Lett. 327 (2000) 181.
[25] H. Peisert, M. Knupfer, T. Schwieger, J.M. Auerhammer, M.S. Golden, J. Fink, J. Appl. Phys. 91 (2002) 4872.
[26] Z. Ahmad, H. Muhammad Sayyad, Physica E 41 (2009) 631.
[27] A.R. Vearey-Roberts, D.A. Evans, Appl. Phys. Lett. 86 (2005) 072105.
[28] G.D. Sharma, S.K. Gupta, M.S. Roy, Thin Solid Films 333 (1998) 176.
[29] S.R. Forrest, M.. Kaplan, P.H. Schmidt, W.L Feldmann, E. Yanowsky, J. Appl. Phys. 41 (1982) 90.
[30] S. Antohe, N. Tomozeiu, S. Gogonea, Phys. status solidi A 125 (1991) 397.
[31] F.E. Jones, B.P. Wood, J.A. Myers, C.D. Hafer, M.C. Lonergan, J. Appl. Phys. 86 (1999) 6431.
[32] T. Kılıçoğlu, M.E Aydın, G. Topal, M.A. Ebeoğlu, H. Saygılı, Synth. Met. 157 (2007) 540.
[33] Ş. Karataş, Ş. Altındal, A. Türüt, A. Özmen, Appl. Surf. Sci. 217 (2003) 250.
[34] I. Dokme, S. Altindal, Semicond. Sci. Technol. 21 (2006) 1053.
[35] Y.P. Song, R.L. Van Meirhaeghe, W.H. Laflere, P. Cardon, Solid-State Electron. 29 (1986) 633.
[36] J.H. Werner, H.H. Guttler, J. Appl. Phys. 73 (1993) 1315.
[37] A. Gumus, A. Trust, N. Yalcin, J. Appl. Phys. 91 (2002) 245.
[38] S. Bandyopadyay, A. Battacharya, S.K. Sen, J. Appl. Phys. 85 (1991) 3671.
[39] M.C. Lonergan, F.E. Zones, J. Chem. Phys. 115 (2001) 433.
[40] R.T. Tung, Phys. Rev. B 45 (1992) 13509.
[41] H. Cetin, E. Ayyildiz, Semicond. Sci. Technol. 20 (2005) 625.
[42] A. Ashok Kumar, V. Janardhanam, V. Rajagopal Reddy, P. Narasimha Reddy. Superlattices Microstruct. 45 (2009) 22.
[43] K.H. Drexhage, in: F.P. Schäfer (Ed.), Topics in Applied Physics, vol. 1, Springer-Verlag, Berlin, 1990, p. 155.
[44] A.O. Marcano, I. Urdaneta, Appl. Phys. B 72 (2001) 207.
[45] S.M. Sze, Physics of Semiconductor Devices, 2nd ed. Wiley, New York, 1981.
[46] E.H. Rhoderick, R.H. Williams, Metal–Semiconductor Contacts, Clarendon, Oxford, 1988.
[47] C. Coskun, M. Biber, H. Efeoglu, Appl. Surf. Sci. 211 (2003) 363.
[48] M. Çakar, N. Yıldırım., Ş. Karataş, C. Temirci, A. Türüt, J. Appl. Phys 100 (2006) 74505.
[49] S.R. Forrest, M.. Kaplan, P.H. Schmidt, W.L Feldmann, E. Yanowsky, J. Appl. Phys. 41 (1982) 90.
[50] Ş. Karataş, M. Çakar, Synth. Met. 159 (2009) 247.
[51] R.F Schmitsdorf, T.U Kampen, W Mönch, Surf. Sci 324 (1997) 249.
[52] R.T Tung, Mater. Sci. Eng. R 35 (2001) 1.
[53] H. Altuntaş, Ş. Altındal, H. Shtrikman, S. Özçelik, Microelectron. Reliab. 49 (2009) 904.
[54] S Chand, J. Kumar, Semicond. Sci. Technol. 11 (1996) 1203.
[55] S Karatas, S Altındal, M. Cakar, Physica B 357 (2005) 386.
[56] MK Hudait, SB. Krupanidhi, Solid-State Electron. 44 (2000) 1089.
[57] A Gumus, A Turut, N. Yalcin, J. Appl. Phys. 91 (2002) 245.
[58] Ş. Karataş, Ş. Altındal, Mater. Sci. Eng. B 122 (2005) 133.
[59] J. Osvald, Semicond. Sci. Technol. 18 (2003) L24.
[60] G.P. Ru, R.L. Van Meirhaeghe, S. Forment, Y.L. Jiang, X.P. Qu, S. Zhu, B.Z. Li, Solid State Electron. 49 (2005) 606.
[61] O. Demircioglu, S. Karatas, N. Yıldırım, O.F. Bakkaloglu, A. Turut, J. Alloys Compd. 509 (2011) 6433.
[62] O. Gullu, A. Turut. J. Alloys Compd. 509 (2011) 571.
[63] M. Biber, Physica B 325 (2003) 138.
[64] Zs.J. Horvath, Solid State Electron. 39 (1996) 176.
[65] J.H. Werner, H.H. Güttler, J. Appl. Phys. 69 (1991) 1522.
[66] S. Chand, J. Kumar, Semicond. Sci. Technol. 10 (1995) 1680.
[67] P.G. Mc Cafferty, A. Sellai, P. Dawson, H. Elasd, Solid State Electron. 39 (1996) 583.
[68] T. Karstens, K. Kobs, J. Phys. Chem. 84 (14) (1980) 1871.